

# The Line Polarization Within a Giant Ly $\alpha$ Nebula

Moire K. M. Prescott<sup>1,2</sup>, Paul S. Smith<sup>2</sup>, Gary D. Schmidt<sup>2,3</sup>, and Arjun Dey<sup>4</sup>

## ABSTRACT

Recent theoretical work has suggested that Ly $\alpha$  nebulae could be substantially polarized in the Ly $\alpha$  emission line, depending on the geometry, kinematics, and powering mechanism at work. Polarization observations can therefore provide a useful constraint on the source of ionization in these systems. In this Letter, we present the first Ly $\alpha$  polarization measurements for a giant Ly $\alpha$  nebula at  $z \approx 2.656$ . We do not detect any significant linear polarization of the Ly $\alpha$  emission:  $P_{Ly\alpha} = 2.6 \pm 2.8\%$  (corrected for statistical bias) within a single large aperture. The current data also do not show evidence for the radial polarization gradient predicted by some theoretical models. These results rule out singly scattered Ly $\alpha$  (e.g., from the nearby AGN) and may be inconsistent with some models of backscattering in a spherical outflow. However, the effects of seeing, diminished signal-to-noise ratio, and angle averaging within radial bins make it difficult to put strong constraints on the radial polarization profile. The current constraints may be consistent with higher density outflow models, spherically symmetric infall models, photoionization by star formation within the nebula or the nearby AGN, resonant scattering, or non-spherically symmetric cold accretion (i.e., along filaments). Higher signal-to-noise ratio data probing to higher spatial resolution will allow us to harness the full diagnostic power of polarization observations in distinguishing between theoretical models of giant Ly $\alpha$  nebulae.

*Subject headings:* galaxies: formation — galaxies: high-redshift — galaxies: evolution — techniques: polarimetric

---

<sup>1</sup>TABASGO Postdoctoral Fellow; Department of Physics, Broida Hall, Mail Code 9530, University of California, Santa Barbara, CA 93106; mkpresco@physics.ucsb.edu

<sup>2</sup>Steward Observatory, University of Arizona, 933 North Cherry Avenue, Tucson, AZ 85721

<sup>3</sup>National Science Foundation, 4201 Wilson Boulevard, Arlington, VA 22230, USA

<sup>4</sup>National Optical Astronomy Observatory, 950 North Cherry Avenue, Tucson, AZ 85719

## 1. Introduction

Very large ( $\sim 100$  kpc) gaseous nebulae, detectable in the high-redshift universe by their spatially extended, luminous Ly $\alpha$  emission, have received substantial attention as the possible sites of ongoing galaxy formation. The question of what powers these Ly $\alpha$  nebulae (colloquially known as Ly $\alpha$  ‘blobs’) has been a subject of keen interest since this class of objects was first discovered more than a decade ago (e.g., Francis et al. 1996; Fynbo et al. 1999; Keel et al. 1999; Steidel et al. 2000), because the origin of the Ly $\alpha$  presumably holds valuable insight into the dominant physical process at work in these complex regions. Observational studies have uncovered evidence that some Ly $\alpha$  nebulae are powered by gravitational cooling radiation (Nilsson et al. 2006; Smith et al. 2008), others by AGN, star formation, or some combination (e.g., Basu-Zych & Scharf 2004; Geach et al. 2009, 2007; Matsuda et al. 2007; Dey et al. 2005; Prescott et al. 2009). Theoretical studies have explored the possibilities of powering by superwind outflows and gravitational cooling radiation (Taniguchi & Shioya 2000; Taniguchi et al. 2001; Dijkstra & Loeb 2009; Goerdt et al. 2010; Faucher-Giguere et al. 2010). However, the uncertainty regarding the degree of obscuration and internal geometry coupled with large uncertainties in the modeling of Ly $\alpha$  radiative transfer has left our understanding of the Ly $\alpha$  nebula phenomenon confused and incomplete. Additional constraints are therefore needed to shed new light on the question of what powers the Ly $\alpha$  emission. In this Letter, we present the first constraints on the Ly $\alpha$  polarization in a giant Ly $\alpha$  nebula.

The observable Ly $\alpha$  polarization from an astrophysical cloud is governed by two important factors (see Lee & Ahn 1998; Loeb & Rybicki 1999; Rybicki & Loeb 1999; Dijkstra & Loeb 2008). First, since Ly $\alpha$  is a resonance line and the primary recombination line of the most abundant element in the universe, Ly $\alpha$  radiative transfer is dominated in most contexts by resonant scattering. Ly $\alpha$  photons are repeatedly absorbed and reemitted by neutral H atoms until they are either destroyed via absorption by dust grains or escape the cloud. Due to thermal motions of the absorbing atoms, photons execute a random walk in both frequency and physical space (e.g., Harrington 1973; Neufeld 1990; Loeb & Rybicki 1999) and are most able to escape an optically thick cloud when they have scattered into the wing of the line profile. Kinematic offsets within the gas - e.g., due to the Hubble expansion, outflows, or infall - can help shift the Ly $\alpha$  photons out of resonance and allow them to escape more readily.

The second important consideration is the processes that might lead to linear polarization of the observed Ly $\alpha$  emission. In pure Rayleigh scattering, the phase function is such that a photon is twice as likely to scatter forward or backward as it is to scatter at a  $90^\circ$  angle, but the polarization is highest for photons that scatter at  $90^\circ$ . Therefore, light

that is initially unpolarized can be highly polarized by scattering off neutral atoms if scattered through large angles. In the case of Ly $\alpha$  scattering, the phase function and degree of polarization qualitatively resemble the case of pure Rayleigh scattering, but the details must be calculated quantum mechanically (e.g., Brandt & Chamberlain 1959; Stenflo 1980; Brasken & Kyrola 1998). A key result is that Ly $\alpha$  scattering in the wing of the line profile yields polarization that is three times higher than Ly $\alpha$  scattering in the line core (Stenflo 1980). Thus, those photons that are most likely to escape (those in the line wing) are also those with the highest polarization. If, after the photons have been polarized, however, they remain trapped in an optically thick cloud, they will resonantly scatter many more times. Since polarization is more likely to be destroyed than preserved in any subsequent scattering event, the highest polarization results from single scattering; as a general rule, the *more* photons scatter, the *less* polarization will be observed. Robust predictions for more complex scenarios require detailed simulations because the ionization state and optical thickness of the cloud, its kinematics, and its geometry will all affect the degree of polarization.

A number of theoretical papers have modeled the expected level of polarization in the Ly $\alpha$  line under a variety of astrophysical scenarios. Focusing first on the pre-reionization epoch, Rybicki & Loeb (1999) showed that a cosmological Ly $\alpha$ -emitting source embedded within the neutral intergalactic medium (IGM) should produce high levels of polarization in the Ly $\alpha$  emission line and that the polarization should increase with radius from the source. At small radii, where photons are scattered many times before they shift out of resonance and escape, the polarization is predicted to be low ( $\sim 14\%$ ). Photons that reach large distances from the source, however, have typically been scattered in one large jump and are traveling roughly radially. The Hubble expansion has shifted them into the wing of the line and their last scattering event has put them on a course to the observer, i.e.  $\sim 90^\circ$  scattering, resulting in higher polarization ( $\sim 32 - 60\%$ ).

In the post-reionization epoch, the situation is somewhat more complicated, and simulations have thus far focused on spherically symmetric geometries. Dijkstra & Loeb (2008) showed that in the case of backscattered radiation in a spherical galactic outflow, the Ly $\alpha$  polarization is predicted to increase strongly with radius to levels as high as  $\sim 40\%$ , depending on the assumed HI column density. The high polarization occurs because the kinematic offset of the gas shifts the photons out of resonance and into the wing of the line, where the induced polarization is higher and where a substantial fraction are able to escape after only one scattering event. The radial increase stems from the fact that photons seen from larger radii have scattered through larger angles in order to reach the observer. In spherically symmetric, collapsing, optically thick clouds, the situation can be similar to that of a spherical outflow, with polarization increasing as a function of radius to values as high as  $\sim 35\%$  (Dijkstra & Loeb 2008). While photons undergo multiple scatterings in this case,

they do so in the line wing where polarization is higher. The radial polarization profile is related to the fact that the Ly $\alpha$  radiation field is increasingly anisotropic with radius; photons emerging from large radii were preferentially traveling radially outward prior to scattering, leading to larger scattering angles and higher polarization. Finally, in the case of resonant scattering in the IGM, the Ly $\alpha$  photons scatter a greater number of times and do so in the core rather than in the wing of the line, yielding lower polarization ( $\sim 2 - 7\%$ ; Dijkstra & Loeb 2008). Dust was assumed to be minimal in these calculations, but in the presence of significant amounts of dust the polarization signature could be higher because the more highly polarized photons are also the ones that scatter the least and are therefore more likely to escape before they are destroyed. Although these predicted polarization levels are encouraging from an observational perspective, it is important to remember that they were derived for the case of spherical symmetry and for specific choices of HI column density and velocity profile; in more complicated scenarios, e.g., cold accretion along filaments, the polarization may be substantially lower (Dijkstra & Loeb 2009). The Ly $\alpha$  polarization from these more complex scenarios has yet to be rigorously modeled.

The existing theoretical predictions have thus far lacked an observational response. In this Letter, we present the first constraints on the Ly $\alpha$  polarization within a giant Ly $\alpha$  nebula. In Section 2, we discuss our observations and data reduction approach. Section 3 presents our results and discusses the implications of our finding that the measured polarization of the Ly $\alpha$  emission in this Ly $\alpha$  nebula is low ( $\lesssim 5\%$  overall or  $\lesssim 12\%$  at large radii). Our conclusions are given in Section 4.

## 2. Observations & Reductions

We chose as our target a giant Ly $\alpha$  nebula at  $z \approx 2.656$  (Dey et al. 2005, hereafter LABd05). With a diameter of roughly 150 kpc and a Ly $\alpha$  luminosity of  $\sim 10^{44}$  erg s $^{-1}$ , it is one of the largest and most luminous Ly $\alpha$  nebulae known, making it a prime candidate for follow-up observations. LABd05 was first discovered thanks to its strong Spitzer/MIPS 24 $\mu$ m emission, stemming from an associated obscured AGN that is offset by  $\sim 20$  kpc (projected) from the peak of the Ly $\alpha$  emission (Dey et al. 2005, Prescott et al. 2011, in preparation).

We obtained imaging linear polarimetry centered on the Ly $\alpha$  line using the Bok 2.3m Telescope and the CCD Imaging/Spectropolarimeter, SPOL (Schmidt et al. 1992a), during the nights of 2007 May 13-15 UT. The instrument is a dual-beam polarimeter built around a rotating semi-achromatic half-waveplate and a Wollaston prism. The SPOL field-of-view at the Bok Telescope is  $100 \times 100$  pixels =  $51'' \times 51''$ , which for our observations contained both LABd05 and two nearby sources that allowed us to verify the position of each dithered

frame.

Maximizing the sensitivity of these observations to polarization in the Ly $\alpha$  line required a high throughput narrow-band filter centered at Ly $\alpha$  at the redshift of the nebula. To achieve this, we selected a filter with an intrinsic central wavelength slightly to the red of Ly $\alpha$  but with high throughput ( $\lambda_c = 4481.19\text{\AA}$ , FWHM =  $56.18\text{\AA}$ ,  $T_{max} = 63.83\%$ ), and used the fact that tilting an interference filter relative to the incident beam has the effect of shifting the central wavelength to the blue. Using filter transmission measurements taken at two different angles, we computed the effective dielectric index of refraction of the filter ( $n_l = 2.1$ ) and used the standard relation ( $\lambda = \lambda_c[1 - \frac{\sin^2\theta}{n_l^2}]^{1/2}$ ) to determine that an inclination angle of  $\theta = 15^\circ.4$  would be needed to shift the central wavelength of the filter to match the Ly $\alpha$  line at this redshift ( $\lambda_{Ly\alpha} = 4446\text{\AA}$ ). We designed an aluminum shim to tilt the filter in the SPOL filter holder by this angle during the observations. Tests done using the instrument as a filtered grating spectrometer at the beginning of the run confirmed that the filter bandpass was correctly centered on Ly $\alpha$  at  $z \approx 2.656$ .

Over three nights we obtained  $18 \times 3200\text{s} = 16$  hours of total integration and followed the standard procedure for polarimetric observations with dual-band polarimeters. The observations suffered from light to moderate cirrus and poor seeing of  $1''.5\text{--}2''.3$ , which in turn led to increased guiding errors, but the advantage of dual-beam polarimetric observations is that changes in transmission cancel during the reduction of the data. To derive the Q Stokes parameter, we obtained 2 separate Q integrations with initial  $\lambda/2$  waveplate positions of  $0^\circ$  and  $45^\circ$ , respectively, relative to the instrumental zeropoint. Each Q integration was divided into 4 individual exposures (200s each), one for each of 4 equivalent waveplate positions. After each individual 200s exposure, the shutter was closed, the waveplate was rotated by  $90^\circ$ , and the shutter was reopened to continue the integration. To derive the U Stokes parameter, the same procedure was used to produce 2 separate U integrations but with the initial waveplate position set to  $22^\circ.5$  and  $67^\circ.5$ , respectively. After each Q and U sequence (3200s), the telescope was dithered by  $\sim 1 - 2''$  in order to reduce the effects of flat-field errors on the total flux image.

We reduced the data using IRAF. We subtracted the bias using the overscan region but did not apply a dark correction as the dark current was measured to be negligible ( $\sim 0.3$  counts per pixel in a 300s exposure). Domeflats for each Stokes sequence were stacked and divided by the median value; the resulting flatfield frame was applied to all images. Cosmic rays were removed from individual exposures using *xzap*.<sup>1</sup> The standard IRAF-based reduction package for SPOL (*impolred*, written by G. Schmidt) was applied to the

---

<sup>1</sup>Written by Mark Dickinson (NOAO).

image/waveplate sequences to yield the polarization results.

We determined the instrumental polarization using observations of unpolarized standard stars (GD319, BD+33 2642, and BD+28 4211). As the instrumental polarization was negligible ( $\lesssim 0.1\%$ ), we did not apply any correction to the data. To measure the polarimetric efficiency of the instrument, we observed a Nicol prism illuminated with the flatfield lamp through a pinhole aperture. This effectively simulated an observation of a star with 100% polarization and yielded a polarimetric efficiency measurement for the  $\lambda/2$  waveplate of 97% in this wavelength bandpass. The science data were corrected accordingly. Observations of interstellar polarization standard stars HD 155528 and Hiltner 960 were made to rotate the measured polarization position angle to the equatorial coordinate system (Schmidt et al. 1992b). The dithered offsets between individual frames were calculated using a nearby source within the image and used to shift each exposure prior to generating the final image stacks.

### 3. Results & Discussion

The mean total flux image is shown along with the Q and U Stokes parameter images in Figure 1. The Ly $\alpha$  emission from LABd05 is clearly detected in the total flux image at a signal-to-noise ratio of 36 (16 pix= $8''.2$  diameter aperture). In the case of polarization due to light scattered from the AGN (shown in Figure 1 as a red cross located at a position angle of  $12^\circ.5$  relative to the Ly $\alpha$  peak), we would expect the electric vector position angle of polarization to be aligned roughly E-W across the nebula. We therefore start by measuring the Q and U Stokes parameters within a 16 pix ( $8''.2$ ) diameter circular aperture centered on the peak of the Ly $\alpha$  emission and find that  $P_{obs} = \sqrt{Q^2 + U^2} = 3.8 \pm 2.8\%$ , with the uncertainty ( $\sigma$ ) derived from photon statistics. As a check, we performed the same aperture photometry on the 18 individual (unstacked) Q and U frames and find that the quoted uncertainty yields  $\chi^2$  indices of unity for the mean Stokes parameters derived from these 18 independent measurements. When we correct for statistical bias - an important effect at low polarization signal-to-noise ratios - the polarization from the circular aperture is  $P \approx P_{obs}(1 - (\sigma_{P_{obs}}/P_{obs})^2)^{1/2} = 2.6 \pm 2.8\%$ , where we assume  $\sigma_{P_{obs}} \approx \sigma$  (Wardle & Kronberg 1974).

Our single aperture measurement of LABd05 is consistent with low Ly $\alpha$  polarization ( $\lesssim 5\%$ ). An idealized scenario in which Ly $\alpha$  photons from the obscured AGN that lies to the north are scattering once off a nearby cloud is clearly not allowed by these observations.

In the case of a single source of Ly $\alpha$  photons centrally located within the cloud (e.g., as in the case of spherical outflow or infall), the polarization vectors would be oriented

perpendicular to the radial vector from the center of the nebula (i.e., in concentric rings) and would cancel when measured with a circular aperture covering the entire nebula. We therefore measured the Q and U Stokes parameters within subapertures (Figure 2) and correct the individual subaperture estimates for the position angle of the radial vector to each subaperture. In Figure 2 we plot these rotated Q and U Stokes parameters along with the resulting polarization fraction averaged within bins in radius. Bins were chosen such that each bin has a signal-to-noise ratio of  $\geq 5$  in the total flux image, but we note that the innermost radial bin is compromised by poor seeing. We find that the polarization in each radial bin is consistent with zero and that there is no evidence for a radial polarization gradient.

The lack of significant Ly $\alpha$  polarization when measured in radial subapertures is difficult to interpret due to the effects of seeing, decreased signal-to-noise ratio, and angle averaging within individual bins. To make a fair comparison, we created simulated observations based on the theoretical models of Dijkstra & Loeb (2008): two models of backscattering in a spherical outflow with HI column densities of  $10^{19} \text{ cm}^{-2}$  and  $10^{20} \text{ cm}^{-2}$ , and a model of a spherically symmetric infalling, optically thick cloud. The backscattered outflow model is described in terms of a parameter  $\alpha_c$ , corresponding to the outer edge of the outflow. For the purposes of comparison, we set  $\alpha_c = 5''$  (chosen such that the simulated peak Ly $\alpha$  surface brightness matches that observed for LABd05, after scaling the model appropriately by redshift and luminosity); however, our qualitative results are not sensitive to this choice. The simulated data were convolved with the typical seeing (FWHM =  $2''0$ ) and binned radially in the same way as the actual data. The simulated measurements are overplotted in Figure 2.

The observed upper limit on the polarization at the center of the last radial bin is  $\leq 11.5\%$  ( $1\sigma$ ). Given the effects of seeing and angle averaging, this corresponds to a  $1\sigma$  limit of  $\lesssim 25\%$  on the *intrinsic* polarization at a radius of  $\sim 5''$ . We find that the observed data are marginally inconsistent with the lower density (higher polarization) model of backscattered emission from a spherical outflow, but we cannot rule out higher density outflow scenarios or the case of a spherically symmetric infalling cloud or resonant scattering in the local IGM.

There are two additional possibilities that are likely consistent with low Ly $\alpha$  polarization. The first possibility is Ly $\alpha$  powered by photoionization from extended star formation or the AGN, which would be expected to either be unpolarized (in the optically thin case) or have low polarization similar to the resonant scattering scenario. The second is non-spherically symmetric cold flows: Dijkstra & Loeb (2009) point out that Ly $\alpha$  escaping from one filament is not likely to be polarized by scattering off another due to the low predicted volume filling factor of cold filaments. However, clear observational constraints on the cold

flow phenomenon are not yet available, and rigorous modeling of the expected Ly $\alpha$  polarization in cold flows has yet to be done.

#### 4. Summary

In this Letter, we present the first observational constraints on the Ly $\alpha$  polarization of spatially extended radio-quiet Ly $\alpha$  nebulae. The polarization fraction of the Ly $\alpha$  emission within LABd05 is  $2.6 \pm 2.8\%$  measured using a large circular aperture, which is inconsistent with a simple model of Ly $\alpha$  photons (e.g., from the AGN) singly scattering off a nearby cloud. We see no evidence for a significant polarization gradient as a function of radius, a result that may rule out models predicting high polarization ( $\sim 40\%$ ) from backscattering in a spherical galactic outflow. However, the effects of seeing, decreased signal-to-noise, and angle averaging within radial bins make it difficult to constrain models that result in somewhat lower polarization: higher column density outflow models, spherically symmetric infall models, and models that invoke photoionization, resonant scattering, or cold flows with non-spherically symmetric geometries. These observations provide the first constraint on the Ly $\alpha$  polarization of giant Ly $\alpha$  nebulae, but as the radial polarization profile is important for distinguishing between models, unleashing the full diagnostic power of polarization observations of giant Ly $\alpha$  nebulae will require higher signal-to-noise ratio data and analysis at higher spatial resolution.

The authors are very grateful to a number of people for assistance with the imaging polarimetry observations, in particular Joseph Scumaci in the Steward Observatory Machine Shop for manufacturing the custom-designed filter shim and Heidi Schweiker at NOAO for tracing the narrow-band filter bandpass on short notice, allowing us to measure the index of refraction. We thank Tony Misch, Mike Bolte, Buell Jannuzi, and the University of California / Lick Observatory for their assistance in making the narrow-band filter available for these polarimetric observations. The authors are grateful to Kristian Finlator, Mark Dijkstra, and an anonymous referee for many helpful discussions and suggestions that improved the paper. The authors would also like to thank Mark Dijkstra for sending his theoretical model results. M. P. was supported by an NSF Graduate Research Fellowship and a TABASGO Prize Postdoctoral Fellowship. Partial support for M. P. was provided by NASA, through a grant (for program GO#10591) from the Space Telescope Science Institute, which is operated by the Association of Universities for Research in Astronomy (AURA) under NASA contract NAS 5-26555. A. D.'s research is supported by NOAO, which is operated by AURA under cooperative agreement with the National Science Foundation.

## REFERENCES

- Basu-Zych, A., & Scharf, C. 2004, *The Astrophysical Journal*, 615, L85
- Brandt, J. C., & Chamberlain, J. W. 1959, *The Astrophysical Journal*, 130, 670
- Brasken, M., & Kyrola, E. 1998, *Astronomy and Astrophysics*
- Dey, A., et al. 2005, *The Astrophysical Journal*, 629, 654
- Dijkstra, M., & Loeb, A. 2009, *Monthly Notices of the Royal Astronomical Society*, 400, 1109
- Dijkstra, M., & Loeb, A. 2008, *Monthly Notices of the Royal Astronomical Society*, 386, 492
- Faucher-Giguere, C. A., Keres, D., Dijkstra, M., Hernquist, L., & Zaldarriaga, M. 2010, eprint arXiv:1005.3041
- Francis, P. J., et al. 1996, *The Astrophysical Journal*, 457, 490
- Fynbo, J. U., Møller, P., & Warren, S. J. 1999, *Monthly Notices of the Royal Astronomical Society*, 305, 849
- Geach, J. E., Smail, I., Chapman, S. C., Alexander, D. M., Blain, A. W., Stott, J. P., & Ivison, R. J. 2007, *The Astrophysical Journal*, 655, L9
- Geach, J. E., et al. 2009, *The Astrophysical Journal*, 700, 1
- Goerdt, T., Dekel, A., Sternberg, A., Ceverino, D., Teyssier, R., & Primack, J. R. 2010, *Monthly Notices of the Royal Astronomical Society*, -1, no
- Harrington, J. P. 1973, *Monthly Notices of the Royal Astronomical Society*, 162
- Keel, W. C., Cohen, S. H., Windhorst, R. A., & Waddington, I. 1999, *The Astronomical Journal*, 118, 2547
- Lee, H.-W., & Ahn, S.-H. 1998, *The Astrophysical Journal*, 504, L61
- Loeb, A., & Rybicki, G. B. 1999, *The Astrophysical Journal*, 524, 527
- Matsuda, Y., Iono, D., Ohta, K., Yamada, T., Kawabe, R., Hayashino, T., Peck, A. B., & Petitpas, G. R. 2007, *The Astrophysical Journal*, 667, 667
- Neufeld, D. A. 1990, *The Astrophysical Journal*, 350, 216

- Nilsson, K. K., Fynbo, J. P. U., Møller, P., Sommer-Larsen, J., & Ledoux, C. 2006, *Astronomy and Astrophysics*, 452, L23
- Prescott, M. K. M., Dey, A., & Jannuzi, B. T. 2009, *The Astrophysical Journal*, 702, 554
- Rybicki, G. B., & Loeb, A. 1999, *The Astrophysical Journal*, 520, L79
- Schmidt, G. D., Elston, R., & Lupie, O. L. 1992a, *The Astronomical Journal*, 104, 1563
- Schmidt, G. D., Stockman, H. S., & Smith, P. S. 1992b, *The Astrophysical Journal*, 398, L57
- Smith, D. J. B., Jarvis, M. J., Lacy, M., & Martínez-Sansigre, A. 2008, *Monthly Notices of the Royal Astronomical Society*, 389, 799
- Steidel, C. C., Adelberger, K. L., Shapley, A. E., Pettini, M., Dickinson, M., & Giavalisco, M. 2000, *The Astrophysical Journal*, 532, 170
- Stenflo, J. O. 1980, *Astronomy and Astrophysics*, 84, 68
- Taniguchi, Y., & Shioya, Y. 2000, *The Astrophysical Journal*, 532, L13
- Taniguchi, Y., Shioya, Y., & Kakazu, Y. 2001, *The Astrophysical Journal*, 562, L15
- Wardle, J. F. C., & Kronberg, P. P. 1974, *The Astrophysical Journal*, 194, 249

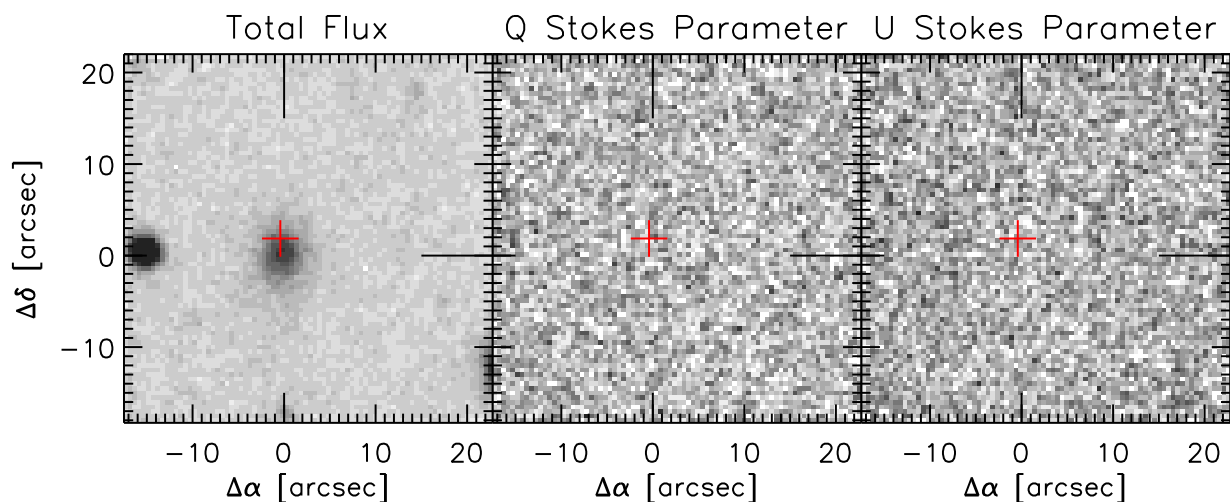


Fig. 1.— Imaging polarimetry of LABd05. The position of the  $\text{Ly}\alpha$  emission peak is indicated by the outer black crosshairs; the position of the obscured AGN is shown as a red cross. The lefthand panel shows the total flux image, and the middle and righthand panels give the Q and U Stokes parameter images. The spatially extended  $\text{Ly}\alpha$  emission is clearly visible in the total flux image ( $\approx 36\sigma$  in a  $8''.2$  diameter aperture) but no polarization is detected ( $2.6\pm 2.8\%$ ).

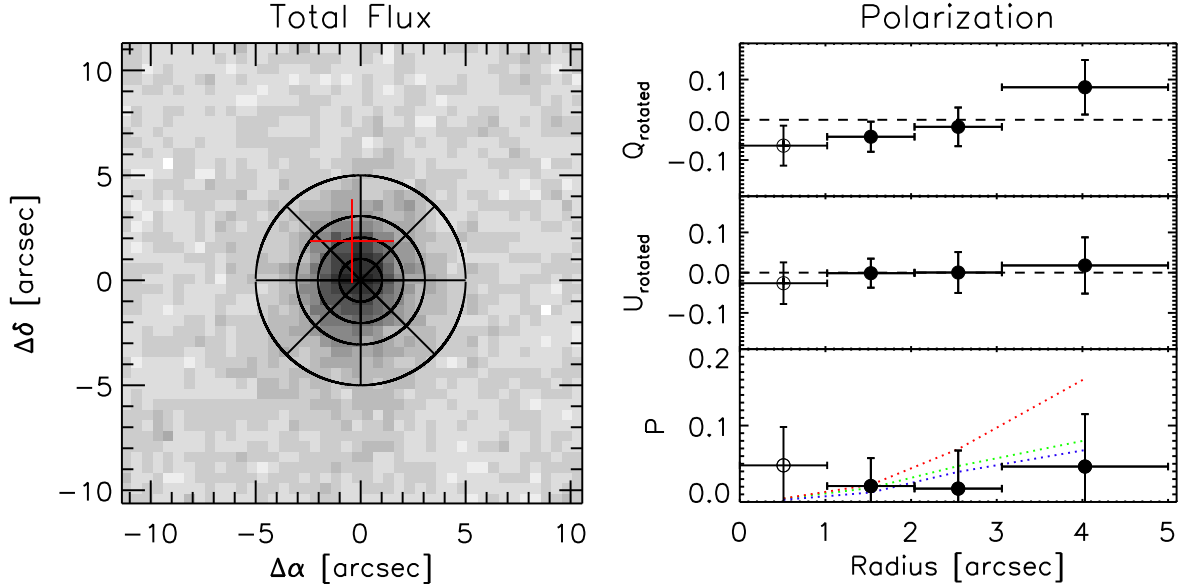


Fig. 2.— (Left) Subapertures used to measure the radial polarization profile are shown overlaid on the total flux image. The position of the obscured AGN is shown (red cross) at a position angle of  $12^{\circ}5$  relative to the center of the Ly $\alpha$  nebula. (Right) Rotated Q and U Stokes parameters and the resulting polarization fraction measured within radial bins using a weighted mean and corresponding error. Measurements for the innermost radial bin are compromised by poor seeing and are denoted with open circles. Simulated results based on theoretical models are overplotted (dotted lines). Models of backscattering in a spherical outflow - for column densities of  $N_{HI} = 10^{19} \text{ cm}^{-2}$  (red) and  $10^{20} \text{ cm}^{-2}$  (green) - and a spherical infall model (blue) are shown. Our observations put an upper limit on the observed polarization of  $\lesssim 12\%$  ( $1\sigma$ ) at large radii, corresponding to an *intrinsic* polarization limit of  $\lesssim 25\%$ .